Chem Biol Drug Des 2012; **80:** 107–113

Research Article

doi: 10.1111/j.1747-0285.2012.01384.x

Discovery of Novel Acyl Coenzyme A: Cholesterol Acyltransferase Inhibitors: Pharmacophore-Based Virtual Screening, Synthesis and Pharmacology

Mahesh T. Chhabria[1,*], Pathik S. Brahmkshatriya[1], Bhushan M. Mahajan[1], Urvesh B. Darji[1] and Gaurang B. Shah[2]

[1]Department of Pharmaceutical Chemistry, L. M. College of Pharmacy, Navrangpura, Ahmedabad 380 009, Gujarat, India
[2]K. B. Institute of Pharmaceutical Education and Research, Gh-6, Sector-23, Gandhinagar 382 023, Gujarat, India
**Corresponding author: Mahesh T. Chhabria, mahesh.chhabria@rediffmail.com*

The present study describes ligand-based pharmacophore modeling of a series of structurally diverse acyl coenzyme A cholesterol acyltransferase inhibitors. Quantitative pharmacophore models were generated using HypoGen module of Discovery Studio 2.1, whereby the best pharmacophore model possessing two hydrophobic, one ring aromatic, and one hydrogen bond acceptor feature for inhibition of acyl coenzyme A cholesterol acyltransferase showed a very good correlation coefficient (r = 0.942) along with satisfactory cost analysis. Hypo1 was also validated by test set and cross-validation methods. Developed models were found to be predictive as indicated by low error values for test set molecules. Virtual screening against Maybridge database using Hypo1 was performed. The two most potent compounds (47 and 48; predicted IC_{50} = 1 nM) of the retrieved hits were synthesized and biologically evaluated. These compounds showed 86% and 88% inhibition of acyl coenzyme A cholesterol acyltransferase (at 10 μg/mL) with IC_{50} value of 3.6 and 2.5 nM, respectively. As evident from the close proximity of biological data to the predicted values, it can be concluded that the generated model (Hypo1) is a reliable and useful tool for lead optimization of novel acyl coenzyme A cholesterol acyltransferase inhibitors.

Key words: ACAT inhibitors, cost analysis, predictive pharmacophore, validation, virtual screening

Received 23 July 2011; revised 28 January 2012 and accepted for publication 25 February 2012

Coronary heart disease (CHD) is the major cause of death in most of the western countries and atherosclerosis is the leading risk factor for its development (1,2). Hyperlipidemia is associated with the increased levels of serum cholesterol, which is the most significant risk factor for the development of atherosclerosis. An attractive target for hyperlipidemia is inhibition of acyl coenzyme A cholesterol acyltransferase (ACAT), an enzyme which catalyzes cholesterol esterification and plays an important role in lipoprotein assembly, dietary cholesterol absorption, and intracellular cholesterol metabolism (3). Two types of ACAT enzymes, viz., ACAT-1 and ACAT-2 have been identified in various mammals including human and mouse. ACAT-1 can accumulate in macrophages and smooth muscle cells to produce foam cells, leading to plaque initiation and atherosclerotic progression (4). On the other hand, the selective distribution of ACAT-2 in the endoplasmic reticulum of liver and intestine seems to suggest that this isoenzyme could operate in a specialized manner, for example in intestinal cholesterol absorption and in lipoprotein secretion (4). In the small intestine, ACAT facilitates the absorption of exogenous cholesterol, which is incorporated into chylomicrons (5,6). In the liver, ACAT plays an important role in the assembly of very low density lipoprotein (VLDL), which is secreted into the blood (7–9). This clearly suggests that inhibition of ACAT remains to be an attractive target to the medicinal chemists for discovery of new antihyperlipidemic agents.

Pharmacophore generation helps to generate a set of minimal structural features required for biological activity which then can be used as a query tool for virtual screening and database searching for exploration of new chemical scaffolds for diverse therapeutic classes. Pharmacophore models are typically used when some active compounds have been identified, but the three-dimensional (3D) structure of the target protein or receptor is unknown. There are several small molecule ACAT inhibitors reported in the literature, which suggest that pharmacophore modeling could be an alternate method of rational design of ACAT inhibitors. HypoGen is quantitative method for generation of pharmacophore. The HypoGen algorithm tries to find hypotheses that are common among the active compounds of the training set, but do not reflect the inactive ones, thus constructing a model that correlates best with measured activities and that consists of as few features as possible. More information on hypogen can be found in the literature (10–14).

In continuation of our search for a new biological lead with potent ACAT inhibitory properties (15), a pharmacophore study on structurally diverse ACAT inhibitors was carried out to gain better insights into structural requirements for ACAT inhibition.

Materials and Methods

Preparation of data set

For the pharmacophore modeling studies, a set of 46 ACAT inhibitors were selected from the literature (16–31) and divided into a training set (21 molecules, Chart S1) and a test set (25 molecules, Chart S2) based on principles of structural diversity and wide coverage of the activity range (between 0.002 and 230 μM, six orders of magnitude). Structures of all compounds in this study were sketched using the Visualizer module of Discovery Studio 2.1. The CHARMm force field was used for calculation of the potential energy. Energy minimizations of all compounds were done using the Smart Minimizer method, which uses the Steepest Descent method, followed by the conjugate Gradient method for faster convergence towards a local minimum, until the root mean square gradient value becomes smaller than 0.001 kcal/mol followed by geometry optimization using the semi-empirical MOPAC-AM1 method.

Pharmacophore generation

A pharmacophore is a representation of generalized molecular features including 3D [hydrophobic (HY) groups, charges/ionizable groups and hydrogen bond donors/acceptors], 2D (substructures) and 1D (physical or biological properties) aspects that are considered to be responsible for a desired biological activity. Selection of feasible features is very important. Each feature is defined by a chemical function, location and orientation in 3D space, tolerance in location, and weight. HypoGen allows a maximum of five features from a set of eleven features which are hydrogen bond acceptor (HBA), hydrogen bond acceptor lipid (HBAL), hydrogen bond donor (HBD), HY, hydrophobic aliphatic (HYAl), hydrophobic aromatic (HYAr), positively (PC) and negatively (NC) charged, positively (PI) and negatively (NI) ionisable and ring aromatic (RA). Taking into account the chemical features of the compounds included in the training set, three features were selected in the hypothesis generation: hydrogen bond acceptor (HBA), HY, and RA. These three features were used to generate the best ten hypotheses from the training set using a default uncertainty value of 3, representing the ratio of the uncertainty range of measured biological activity against the actual activity for each compound. The minimum and maximum number of features varied to achieve a statistically significant model. The best model was generated using HBA, min 1 and max 3; HY, min 2 and max 2; and RA, min 1 and max 3. The generated pharmacophore has three features and four points, viz. one HBA, two HY, and one RA. The best hypothesis is called as Hypo 1.

Pharmacophore validation

To validate the reliability and accuracy of the generated 3D pharmacophore models, cost analysis, test set activity prediction and Fischer's randomization (Y scrambling) test studies were performed.

Cost analysis

The quality of HypoGen models can be described in terms of fixed cost, null cost, and total cost (32). As a good model, the total cost of any hypothesis should be close to the fixed cost. If a returned cost (total cost) differs from the null hypothesis by 40–60 bits, it is highly probable that the hypothesis has 75–90% chance of representing the true correlation of the data (Discovery Studio 2.1 documentation[a]).

Test set validation

Test set validation is a type of external validation method. In addition to validating the predictive ability of training set molecules, the pharmacophore model should also estimate the activity of new compounds. Therefore, a set of 25 compounds (**22–46**) were included in the test set, which were not included in the training set. These compounds cover wide range of activity range spanning from 0.005 to 97 μM.

Fischer's randomization test

To evaluate the statistical relevance of the model, the Fischer's randomization test was applied. The purpose of the Fischer randomization test is to validate the strong correlation between chemical structures and biological activity. The activity values of the training set molecules are reassigned by randomization using the Fischer's randomization test and new spreadsheets are created. The number of spreadsheets depends on what level of statistical significance one wants to achieve. These randomized spreadsheets should yield hypotheses without statistical significance; otherwise, the original model was also obtained randomly. To achieve a statistical significance level of 95%, 19 random spreadsheets were generated.

Chemistry

Melting points were determined in open capillaries in a microprocessor based melting point apparatus model VMP-D (Veego make) and are uncorrected. Infrared spectra were recorded in KBr using a 8400S Shimadzu Fourier Transform spectrophotometer. NMR Proton Nuclear Magnetic Resonance spectra were taken on Bruker Avance 400 spectrophotometer at 400 MHz and the chemical shifts are given as parts per million (δ ppm) downfield from tetramethylsilane (TMS) as the internal standard. Mass spectra (ESI) were obtained on Perkin–Elmer LC-MS PE Sciex API/65.

General procedure for synthesis of ethyl disubstituted-4-[((2-(phenylcarbonyl)phenyl) carbonyl)oxy]benzoate

To a solution of benzophenone-2-carboxylic acid (**56**) (10 mmol) in dichloromethane (10 mL) at 0 °C, a solution of ethyl 3,5-disubstituted-4-hydroxybenzoate (**55**) (11 mmol) in dichloromethane (10 mL) was added. The reaction mixture was allowed to stir for 15 min at 0 °C after which DMAP (1 mmol) and DCC (11 mmol) were added to the reaction mixture in one lot. The reaction mixture was allowed to stir for another 30 min at room temperature. The precipitates of dicyclohexylurea were filtered off and the filtrate was concentrated under vacuum to afford crude product which was recrystallized using a mixture of methanol–water to afford pure product.

Ethyl 3,5-dibromo-4-({[2-(phenylcarbonyl)phenyl] carbonyl}oxy)benzoate (47)

Off-White solid. Yield: 75%. Mp 130–134 °C; ^{1}H NMR ($CDCl_3$, 400 MHz): 8.40–8.38 (1H, dd; J = 8.8Hz, J = 8.0 Hz) (8.15, 2H, s), 7.80–7.66 (4H, m), 7.56–7.50 (2H, m), 7.42–7.38 (t, 2H; J = 7.6 Hz), 4.40 (2H, q; J = 7.4 Hz), 1.38 (3H, t; J = 7.4 Hz) anal $C_{23}H_{16}Br_2O_5$, Mass calcd. 529.94; MS (ESI+) m/z 531.2 (M + H+; 100%).

Ethyl 3,5-dichloro-4-({[2-(phenylcarbonyl)phenyl] carbonyl}oxy)benzoate (48)

Off-White solid. Yield: 51%. Mp 115–119 °C; ^{1}H NMR ($CDCl_3$, 400 MHz): 8.39–8.38 (1H, dd; J = 8.8 Hz, J = 7.8 Hz), 7.96 (2H, s), 7.81–7.67 (4H, m), 7.56–7.50 (2H, m), 7.43–7.39 (t, 2H; J = 7.5 Hz), 4.36 (2H, q; J = 7.1 Hz), 1.37 (3H, t; J = 7.2 Hz) anal $C_{23}H_{16}Cl_2O_5$, Mass calcd. 442.04; MS (ESI+) m/z 443.4 (M + H+; 100%).

ACAT inhibition assay

The ACAT enzyme inhibitory activity was assayed using the method described by Lada *et al.* (33) with the following modifications. The reaction mixture included 0.03 mL of rat liver microsome fraction, 0.5 mL of KH_2PO_4 buffer (0.2 M, pH 7.4) containing (15 mg/mL) bovine serum albumin, and 0.03 mL of DMSO vehicle with 0.03 mL of test drugs in three different concentrations, viz. 1, 10, 100 μg/mL. The reaction mixture was incubated at 37 °C for 10 min after which 0.02 mL of palmitoyl Co-A (Sigma Aldrich, St Louis, MO, USA) was added, and the reaction was run at 37 °C for 5 min. The reaction was stopped by the addition of 2:1 chloroform-methanol, phases were separated, and the organic phase was concentrated. The residue was dissolved in 0.5 mL of 2-propanol containing 10% Triton X-100, followed by addition of 0.3 mL of free cholesterol decomposition reagent. Both the above-mentioned reagents were part of a commercially available kit (Span Diagnostics, India). The reaction mixture was then incubated at 37 °C for 15 min after which 0.15 mL of cholesteryl ester measurement reagent was added, and the reaction mixture was again incubated at 37 °C for 15 min. The enzyme activity was measured by estimation of the reaction followed from the increase in absorbance at 600 nm.

Results and Discussion

Pharmacophore model

The first HypoGen run was carried out using pharmacophoric parameters, HBA min 1, max 3; HY min 2, max 2 and RA min 1, max 3. FAST conformation generation was applied with the minimum conformation set as 255 and other parameters were kept at their default settings. The model (Model 1) showed relatively good correlation (r = 0.886) between the actual and estimated activity, and a higher difference among the total cost and null cost (Δ = 78.558). The configuration cost was 16.56, as it was <17, it is considered that all the generated hypothesis were not because of the chance correlation. To further improve the cost and correlation coefficients, another HypoGen run (Model 2) was carried out using pharmacophoric features, HBA min 1, max 3; HY min 1, max 2 and RA min 1, max 3. Other parameters were kept the same as described above. The second run resulted in improvement of correlation (r) from 0.886 to 0.912, but an increase in configuration cost from 16.56 to 17.15, having a total cost of 117.664. The model was discarded as the configuration cost exceeded the normal permissible limit of 17. Therefore, to achieve further improvement, another HypoGen run (Model 3) was carried out using pharmacophoric features min 1, max 3; HY min 2, max 2 and RA min 1, max 3. The correlation (r) was found to be 0.942 with a better configuration cost (16.45). The cost analysis shows that total cost, null cost, and fixed cost are 106.014, 176.924 and 88.81 respectively. The difference between total cost and null cost is 70.91 bits, indicating that the generated model exhibits ~90% probability of true correlation. The difference between total cost and fixed cost is 17.203 (<20 indicates good correlation, Discovery Studio 2.1 documentation). The best model was generated using HBA, min 1 and max 3; HY, min 2 and max 2; and RA, min 1 and max 3. The generated pharmacophore is three features and four point pharmacophore, which contains one HBA, two HY and one RA. The best hypothesis is called as Hypo 1. The results for the Hypogen model (Model 3) are shown in Table 1, along with its statistics and cost analysis.

Pharmacophore model validation

Fischer's randomization (CatScramble) study

With the help of the Catscramble program, the experimental activities of compounds in the training set were scrambled randomly and the resulting training set was used for a HypoGen run. The results of the Fischer test are shown in Table 2; the data clearly suggest that none of the generated hypotheses after randomization have a cost value lower than that of Hypo1, and none of the hypotheses had correlation higher than that of the Hypo1. This suggests that there is a 95% chance for the best hypothesis to represent a true correlation in the training set activity data.

Test set validation

Hypo1 was further validated using a test set of 25 compounds which were structurally distinct from those included in the training

Table 1: Results of pharmacophore hypothesis generated using training set molecules (Model 3)[a]

Hypothesis no.	Total cost[a]	Δ Cost	RMSD	Correlation (r)
1	106.014	70.91	1.9038	0.942
2	113.108	63.816	1.4067	0.899
3	114.794	62.13	1.4512	0.893
4	114.976	61.948	1.4582	0.892
5	115.19	61.734	1.5444	0.875
6	115.833	61.091	1.5648	0.872
7	115.89	61.034	1.5308	0.878
8	116.509	60.415	1.5775	0.869
9	116.942	59.982	1.5930	0.867
10	117.291	59.633	1.6085	0.864

[a]Null cost of 10 top-scored hypothesis is 176.924, fixed cost value is 88.811, and configuration cost is 16.45.

set. All the compounds were classified on the bases of their activity scale, as highly active compounds (<0.1 μM denoted by +++), moderately active compounds (0.1–10 μM denoted by ++), and/or inactive compounds (>10 μM denoted by +). As shown in Table 3, all highly active compounds predicted correctly, only two moderately active compounds (**35** and **39**) were predicted to be inactive, and only two inactive compounds (**42** and **44**) were predicted to be moderately active. Furthermore, a regression analysis of the experimental and predicted values of inhibitory activity of the test set compounds gives a very good correlation coefficient of 0.955, indicating a good predictive ability (Figure 1).

Table 2: Results Fischer's randomization test using CatScramble protocol

Hypothetical No.	Total cost	Correlation (*r*)
Hypo 1	106.01	0.9425
Random 1	157.35	0.6207
Random 2	167.86	0.5081
Random 3	129.83	0.8204
Random 4	154.99	0.6182
Random 5	159.32	0.5716
Random 6	122.49	0.8500
Random 7	150.47	0.6356
Random 8	154.57	0.6188
Random 9	156.69	0.6152
Random 10	140.19	0.7128
Random 11	158.15	0.5439
Random 12	142.12	0.7409
Random 13	152.51	0.6239
Random 14	143.78	0.7793
Random 15	141.07	0.7070
Random 16	158.83	0.6200
Random 17	146.68	0.7090
Random 18	150.54	0.6592
Random 19	121.57	0.8390

Database searching

To identify novel and potent ACAT inhibitors, virtual screening was performed using the best flexible database search tool in Discovery Studio 2.1. The best pharmacophore model was used as a query to search a commercial database Maybridge. In the present study, best flexible conformation generation was used to find out the hit from database. Interestingly, over ninety compounds fitted well with features of Hypo1. Results of some of the top hits are summarized in Table 4 along with their predicted IC_{50} and fit values (See Chart S3 for structures). It should be noted that only compounds **47–54** (Table 4) are found to be highly active (estimated IC_{50} < 100 nM) and rest of the compounds, although with good fit values, were only moderately active (IC_{50} > 100 nM). Hence, only the top eight compounds (**47–54**) are shown in Table 4. Pharmacophore mapping of the most potent compound (**2**) with Hypo1 (Model 3) is shown in Figure 2A. Mapping of synthesized compounds (**47** and **48**) are shown in Figure 2B and 2C. The pharmacophoric distances between

Table 3: Actual and estimated activity comparison of test set molecules using Hypo1

Compound No.	Experimental IC_{50} (μM)	Estimated IC_{50} (μM)	Error[a]	Fit value[b]	Experimental scale[c]	Estimated scale
22	0.005	0.001	−5	11.236	+++	+++
23	0.006	0.001	−6	11.27	+++	+++
24	0.01	0.001	−10	11.362	+++	+++
25	0.01	0.001	−10	11.315	+++	+++
26	0.01	0.001	−10	11.44	+++	+++
27	0.012	0.003	−4	10.658	+++	+++
28	0.013	0.001	−13	11.343	+++	+++
29	0.015	0.001	−15	11.2	+++	+++
30	0.022	0.001	−22	11.125	+++	+++
31	0.026	0.001	−26	11.42	+++	+++
32	0.052	0.018	−2.89	9.912	+++	+++
33	0.062	0.007	−8.86	10.323	+++	+++
34	0.53	0.346	−1.53	8.62	++	++
35	0.74	10.832	14.63	7.125	++	+
36	0.79	0.484	−1.63	8.475	++	++
37	1	2.111	2.111	7.835	++	++
38	1.2	2.844	2.37	7.706	++	++
39	8.7	98.875	11.36	6.165	++	+
40	8.8	4.292	−2.05	7.527	++	++
41	12	99.829	8.31	6.161	+	+
42	12	1.411	−8.5	8.01	+	++
43	12	147.164	12.26	5.992	+	+
44	15	0.719	−20.86	8.303	+	++
45	49	747.611	15.26	5.286	+	+
46	97	1926.63	19.86	9.875	+	+

[a]+ means that the estimated IC_{50} is higher than the experimental IC_{50}; means that the estimated IC_{50} is lower than the experimental IC_{50}; a value of 1 indicates that the estimated IC_{50} is equal to the experimental IC_{50}.
[b]Fit value indicates how well the features in the pharmacophore map the chemical features in the molecule.
[c]Activity scale: +++, $IC_{50} \leq 0.01$ μM (highly active); ++, 0.01 μM < $IC_{50} \leq 0.1$ μM (moderately active); +, IC_{50} > 0.1 μM (low active).

the features are shown in Figure 2D. These promising results led us to synthesize and evaluate the two most potent compounds **47** and **48** (Scheme 1) for their ability to inhibit ACAT.

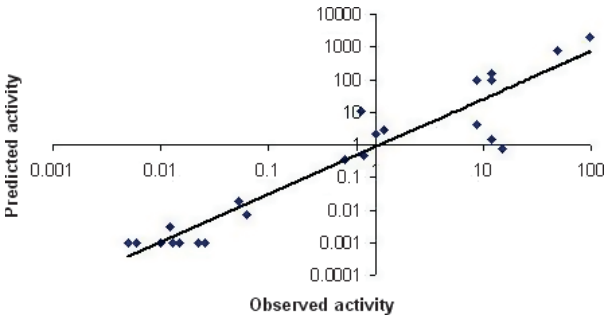

Figure 1: Correlation of experimental versus estimated activities by Hypo1 for the test set.

Table 4: List of compounds retrieved in 3D database searching

Compound No.	Estimated IC_{50} (μM)	Fit value
47	0.001	11.134
48	0.001	11.002
49	0.004	10.565
50	0.013	10.042
51	0.022	9.812
52	0.024	9.782
53	0.056	9.469
54	0.067	9.333

Chemistry

The synthetic route for compounds **47** and **48** is outlined in Scheme 1. Benzophenone-2-carboxylic acid (**56**) was obtained using phthalic anhydride and benzene as starting materials by Friedel Craft's acylation, according to the literature (34). Acid-catalyzed esterification of corresponding acids afforded ethyl 3,5-dichloro 4-hydroxybenzoate (**55a**) and ethyl 3,5-dibromo-4-hydroxybenzoate (**55b**). Coupling of compound **55a** and **55b** with **56** in presence of DCC and DMAP afforded target compounds **47** and **48** respectively.

ACAT inhibitory activity

Both the synthesized compounds were tested for their inhibitory properties toward ACAT extracted from male Sprague-Dawley rat liver microsomes. Their activity, expressed as percentage inhibition at 10 μg/mL, is shown in Table 5. Compound **47** showed 86% inhibition whereas compound **48** showed 88% inhibition of rat liver microsomal ACAT. The IC_{50} values were obtained by the Logit method (35,36) and were determined from the results of at least three independent tests. IC_{50} values of **47** and **48** were found to be 3.6 and 2.5 nM, respectively, which were found to be very close to the predicted value indicating that pharmacophore-based ACAT inhibitor design was a rational protocol in lead generation. Two of the most potent compounds (**47** and **48**) predicted by virtual screening (fit value 11.134 and 11.002, respectively) were found to be highly potent *in vitro* when tested for their ability to inhibit rat liver microsomal ACAT. As expected, the compounds essentially possessed highly lipophilic functionalities (two ester linkages, three phenyl rings; AlogP = 6.199 and 6.367, respectively (37) and a few hydrogen bond acceptor atoms (carbonyl oxygen) which was found to be the key pharmacophoric requirements as predicted by Hyop1. Interestingly,

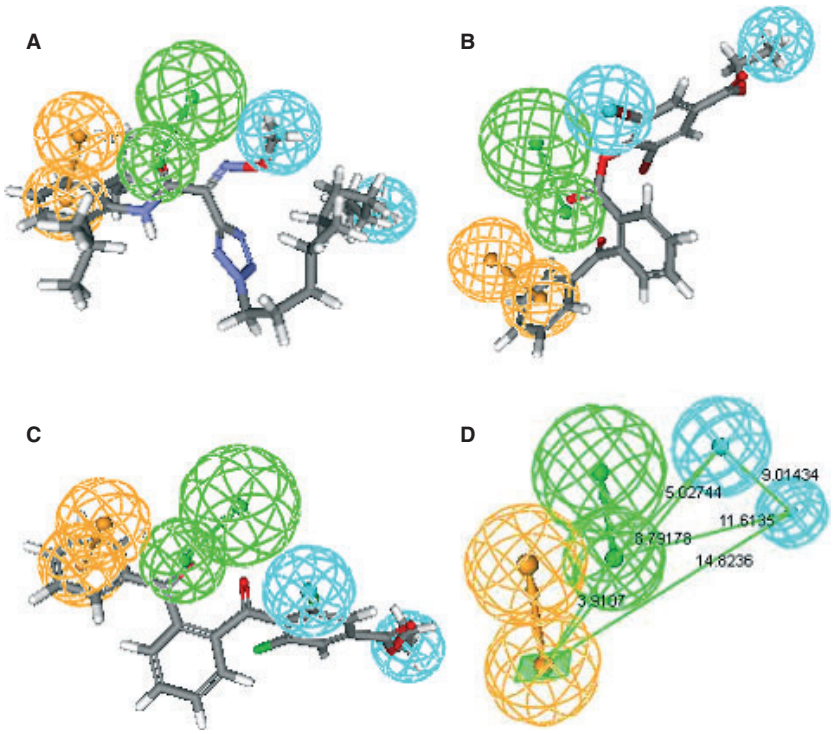

Figure 2: The best Hypogen pharmacophore model mapping (A) With the most active (IC_{50} = 0.002 μM) compound **2**; (B) With the compound **47** (Predicted IC_{50} = 0.001 μM); (C) With the compound **48** (Predicted IC_{50} = 0.001 μM). (D) 3D spatial relationship and pharmacohporic distances of Hypo 1. Pharmacophore features are color coded (green, HBA; orange, ring aromatic and cyan hydrophobic).

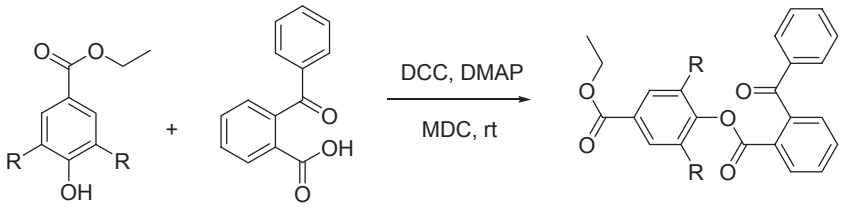

Scheme 1: Synthetic route for the synthesis of target compounds **47** and **48**.

Table 5: Results of ACAT inhibition of synthesized compounds (**47** and **48**)

Compound No.	Conc. (μg/mL)	% Inhibition[a]	Logit[b]	IC_{50} (μM)[c]
47	10	86.2	0.7956	0.0036
48	10	88.14	0.8761	0.0025

[a]% inhibition = [(standard conc. − test conc.)/standard conc.] × 100.
[b]Logit = log [(% inhibition/(100 − % Inhibition)].
[c]pIC_{50} = Logit − logC; where, C is molar concentration.

logP values of both the compounds were found to be very close to that of the well-known ACAT inhibitor CI-976 (logP = 6.17). The target compounds thus stand out as promising novel leads for further structural optimization and pharmacological studies.

Conclusions

In the present study, predictive pharmacophore models were developed for a series of structurally diverse ACAT inhibitors using HypoGen. The best model (Hypo1) has four pharmacophore features viz. one hydrogen bond acceptor, two HY and one RA showed good correlation (r = 0.942). Validation of the generated hypothesis was carried out using cost analysis (Δcost = 70.91; configuration cost = 16.45) and the Fischer randomization test. The predictive ability of generated hypotheses was also checked using a set of 25 test compounds (r = 0.955). Results showed that a majority of compounds were predicted correctly, with lower error values and good fit values. The best hypothesis (Hypo 1; model 3) was used as a 3D query for searching the Maybridge database, which identified structurally diverse scaffolds with activity ranging from 1 to 170 nM as plausible leads for the design of novel ACAT inhibitors. With the help of these lead molecules, several compounds were predicted and planned for the synthesis. Compounds **47** and **48** were synthesized and screened for ACAT inhibitory activity on liver microsomes preparations of male Sprague-Dawley rat. The activity of the synthesized compounds was found to be very close to the predicted activity, suggesting a high predictive ability of the generated pharmacophore model. Binding assays for ACAT subtypes and a lead optimization study of the identified lead molecules are underway in our laboratory.

Acknowledgments

Authors acknowledge University Grants Commission, Govt. of India, for the financial support.

References

1. Chhabria M.T., Brahmkshatriya P.S. (2006) Novel targets for the treatment of atherosclerosis. Curr Opin Invest Drugs;7:820–825.
2. Brahmkshatriya P.S., Chhabria M.T., Jani M.H. (2006) Recent developments in the treatment of atherosclerosis. J Enzyme Inhib Med Chem;21:1–15.
3. Kushwaha R.S., Vandeberg J.F., Rodriguez R., Vandeberg J.L. (2004) Cholesterol absorption and hepatic acyl-coenzyme A:cholesterol acyltransferase activity play major roles in lipemic response to dietary cholesterol and fat in laboratory opossums. Metabolism;53:817–822.
4. Rudel L.L., Lee R.G., Cockman T.L. (2001) Acyl coenzyme A: cholesterol acyltransferase types 1 and 2: structure and function in atherosclerosis. Curr Opin Lipidol;12:121–127.
5. Field F.J., Salome R.G. (1982) Effect of dietary fat saturation, cholesterol and cholestyramine on acyl-CoA: cholesterol acyltransferase activity in rabbit intestinal microsomes. Biochim Biophys Acta;712:557–570.
6. Heider J.G., Pickens C.E., Kelly L.A. (1983) Role of acyl CoA:cholesterol acyltransferase in cholesterol absorption and its inhibition by 57-118 in the rabbit. J Lipid Res;24:1127–1134.
7. Drevon C.A., Engelhorn S.C., Steinberg D. (1980) Secretion of very low density lipoproteins enriched in cholesteryl esters by cultured rat hepatocytes during simulation of intracellular cholesterol esterification. J Lipid Res;21:1065–1071.
8. Khan B., Wilcox H.G., Heimberg M. (1989) Cholesterol is required for secretion of very-low-density lipoprotein by rat liver. Biochem J;258:807–816.
9. Cianflone K.M., Yasruel Z., Rodriguez M.A., Sniderman A.D. (1990) Regulation of apoB secretion from HepG2 cells: evidence for a critical role for cholesteryl ester synthesis in the response to a fatty acid challenge. J Lipid Res;31:2045–2055.
10. Mishra R.K., Singh J. (2010) Generation, validation and utilizaiton of three-dimensional pharmacophore model for EP3 antagonists. J Chem Inf Model;50:1502–1509.
11. Brogi S., Kladi M., Vagias C., Papazafiri P., Roussis V., Tafi A. (2009) Pharmacophore modelling of qualitative prediction of antiestrogenic activity. J Chem Inf Model;49:2489–2497.
12. Krovat E.M., Langer T. (2003) Non-peptide angiotensin II receptor antagonists: chemical feature based pharmacophore identification. J Med Chem;46:716–726.
13. Funk O.F., Kettmann V., Drimal J., Langer T. (2004) Chemical function based pharmacophore generation of Endothelin-A selective receptor antagonists. J Med Chem;47:2750–2760.

14. Barreca M.L., Ferro S., Rao A., Luca L.D., Zappala M., Monforte A.-M., Debyser Z., Witvrouw M., Chimirri A. (2005) Pharmacophore-based design of HIV-1 integrase strand-transfer inhibitors. J Med Chem;48:7084–7088.
15. Chhabria M.T., Mahajan B.M., Brahmkshatriya P.S. (2010) QSAR study of a series of acyl coenzyme A (CoA): cholesterol acyltransferase inhibitors using genetic function approximation. Med Chem Res;???:???–???. Online first, DOI: 10.1007/s00044-010-9413-3.
16. Picard J.A., O'Brien P.M., Sliskovic D.R., Anderson M.K., Bousley R.F., Hemelehle K.L., Krause B.R., Stanfield R.L. (1996) Inhibitors of Acyl-CoA: cholesterol *O*-Acyltransferase. Structure-activity relationships of several series of compounds derived from *N*-chlorosulfonylisocyanate. J Med Chem;39:1243–1252.
17. O' Brien P.M., Sliskocic D.R., Picard J.A., Lee H.T., Purchase C.F., Roth B.D., White A.D. *et al.* (1996) Inhibitors of Acyl-CoA: cholesterol *O*-Acyltransferase. Synthesis and pharmacological activity of (±)-2-dodecyl-phenyl-*N*-(2,4,6,trimethoxy)-2H-tetrazole-5-acetamide and structurally related tetrazole amide derivatives. J Med Chem;39:2354–2366.
18. White A.D., Purchase C.F., Picard J.A., Anderson M.K., Mueller S.B., Bocan T.M.A., Bousley R.F., Hammelehle K.L., Krause B.R., Lee P., Stanfield R.L., Reindel J.F. (1996) Heterocyclic amides: inhibitors of Acyl-CoA:cholestrol *O*-Acyltransferase with hypocholesterolemic activity in several species and antiatherosclerotic activity in the rabbit. J Med Chem;39:3908–3919.
19. Sliskovic D.R., Picard J.A., O'Brien P.M., Liao P., Roark W.H., Roth B.D., Anderson M.A. *et al.* (1998) α–Substituted malonester amides: tools to define the relationship between ACAT inhibitors and adrenal toxicity. J Med Chem;41:682–690.
20. Giovannoni M.P., Piaz V.D., Kwon B.M., Kim Y.K., Toma L., Barlocco D., Bernini F., Canavesi M. (2001) 5-6-Diphenylpyridazine derivatives as Acyl- CoA:cholesterol acyltransferase inhibitors. J Med Chem;44:4292–4295.
21. Ohishi K., Aiyama R., Hatano H., Yoshida Y., Wada Y., Yokai W., Sawada H., Watanabe T., Yokokura T. (2001) Strucure-activity relationships of *N*-(3,5-dimethoxy-4-*n*-octyloxycinnamoyl)-N9-(3,4-dimethylphenyl)piperazine and analogues as inhibitors of Acyl CoA:cholesterol O-Acyltransferase. Chem Pharm Bull;49:830–839.
22. Toma L., Giovannoni M.P., Vergelli C., Piaz V.D., Kwon B.M., Kim Y.K., Gelain A., Barlocco A. (2002) Novel 3-arylamino- and 3-cycloalkylamino 5,6-diphenyl-pyridazines active as ACAT Inhibitors. Arch Pharm Pharm Med Chem;11:563–566.
23. Lee H.T. (1996) Sulphonate ACAT inhibitors. U. S. Patent 5,510,379, April, 23.
24. Lee H.T. (1997) Tetrazole Alkyl Amide ACAT Inhibitors. U. S. Patent 5,646,170. July, 8.
25. Dugar S. (1994) 1,2-Disubstituted Ethyl Amides as Inhibitors of ACAT. WO94/06784, March, 31.
26. Lee H.T., Picard J.A., Sliskovic D.R. (1996) β–Carboxy Sulfonamide ACAT Inhibitors. U. S. Patent 5,491,170, February, 13.
27. Roark W.H. (2000) Phosphonamide ACAT inhibitors. U. S. Patent 6,017,905, January, 25.
28. O'Brien P.M., Sliskovic D.R. (1995) Amide tetrazole ACAT inhibitors. U. S. Patent 5,461,049, October, 24.
29. Higley C., Wilde R.G., Maduskuie T.P., Johnson A.L., Pennev P., Billheimer J.T., Robinson C.S., Gillies P.J., Wexler R.R. (1994) Acyl CoA:cholesterol Acyltransferase (ACAT) inhibitors: synthesis and structure–activity relationship studies of a new series of trisubstituted imidazoles. J Med Chem;37:3511–3522.
30. Dugar S., Clader J.W., Burrier R.E., Kogan T.P. (1993) N-Oleoyl-1,2,3,4- tetrahydroquinolines as confomationally restricted inhibitors of Acyl-CoA: cholesterol Acyl Transferase (ACAT). Bioorg Med Chem Lett;3:571–576.
31. Boswell G.A., Li H.Y., Delucca I., Billheimer J.T., Drummond S., Gillies P.J., Robinson C. (1996) Novel 4,4-bis(trifluoromethyl) imidazoles as stereospecific and orally active Acyl CoA: cholesterol Acyltransferase (ACAT) inhibitors and antihypercholesterolemic agents. Bioorg Med Chem Lett;6:885–888.
32. Debnath A.K. (2002) Pharmacophore mapping of a series of 2,4-diamino-5-deazapteridine inhibitors of Mycobacterium avium complex dihydrofolate reductase. J Med Chem;45:41–53.
33. Largis E., Wang C., BeVaries V., Schaffe F. (2004) CL277,082; A novel inhibitor of ACAT catalysed cholesterol esterification and cholesterol absorption. J Lipid Res;45:396–401.
34. Furniss B.S., Hannaford A.J., Smith P.W.G., Tatchell A.R. (2006) Vogel's Textbook of Practical Organic Chemistry, 5th edn. London, UK: Pearson Publishing Corp.
35. Wang Y., Ai J., Wang Y., Chen Y., Wang L., Liu G., Geng M., Zhang A. (2011) Synthesis and c-Met kinase inhibition of 3,5-disubstituted and 3,5,7-trisubstituted quinolines: identification of 3-(4-acetylpiperazin-1-yl)-5-(3-nitrobenzylamino)-7- (trifluoromethyl)quinoline as a novel anticancer agent. J Med Chem;54:2127–2142.
36. Manvar A., Malde A., Verma J., Virsodia V., Mishra A., Upadhyay K., Acharya H., Coutinho E., Shah A. (2008) Synthesis, antitubercular activity and 3D-QSAR study of coumarin-4-acetic acid benzylidene hydrazides. Eur J Med Chem;43:2395–2403.
37. Ghose A.K., Crippen G. (1986) Atomic physicochemical parameters for three-dimensional structure-directed quantitative structure-activity relationships I. Partition coefficient as a measure of hydrophobicity. J Comp Chem;7:565–577.

Notes

[a]Accelrys Inc., San Diego, CA, USA.

Supporting Information

Additional Supporting Information may be found in the online version of this article:

Chart S1. Chemical structures of training set compounds (**1**–**21**) with their IC_{50} values (in parentheses).

Chart S2. Chemical structures of test set compounds (**22**–**46**) with their IC_{50} values (in parentheses).

Chart S3. Structures of hits (**47**–**54**) found as query in virtual screening.

Please note: Wiley-Blackwell is not responsible for the content or functionality of any supporting materials supplied by the authors. Any queries (other than missing material) should be directed to the corresponding author for the article.